

Lensing and high- z supernovae surveys

Daniel E. Holz

Enrico Fermi Institute and Department of Physics
 University of Chicago
 5640 South Ellis Avenue
 Chicago, IL 60637-1433
 deholz@rainbow.uchicago.edu

ABSTRACT

Gravitational lensing causes the distribution of observed brightnesses of standard candles at a given redshift to be highly non-gaussian. The distribution is strongly, and asymmetrically, peaked at a value less than the expected value in a homogeneous Robertson-Walker universe. Therefore, given any small sample of observations in an inhomogeneous universe, the most likely observed luminosity is at flux values less than the Robertson-Walker value. This paper explores the impact of this systematic error due to lensing on surveys predicated on measuring standard candle brightnesses. We re-analyze recent results from the high- z supernovae team (Riess et al. 1998a), taking lensing into account in the analysis. We find that the best-fit model remains unchanged (at $\Omega_m = 0$, $\Omega_\Lambda = 0.45$), but the confidence contours change size and shape, becoming larger (and thus allowing a broader range of parameter space) and drooping towards higher values of matter density, Ω_m (or correspondingly, lower values of the cosmological constant, Ω_Λ). For example, neglecting lensing, the $\Omega_m = 0.5$, $\Omega_\Lambda = 0.5$ model is more than 2σ away from the best fit. When lensing effects are included, this cosmology is at 1σ .

Subject headings: cosmology: theory—cosmology: observations—gravitational lensing—methods: numerical—supernovae: general

1. INTRODUCTION

Recently there has been great activity in determining cosmological parameters based on the observations of type 1a supernovae at high redshifts (Perlmutter et al. 1998, 1997; Riess et al. 1998a; Schmidt et al. 1998). The peak flux of these supernovae is thought to be known to within 0.15 mag (Hamuy et al. 1996; Riess, Press, & Kirshner 1996), making them excellent standard candles with which to measure the luminosity distance—redshift relation. As this relation is dependent upon the cosmological parameters (H_0 , Ω_m , Ω_Λ), it is possible to infer the values of these parameters from supernovae 1a observations. Two independent groups (Perlmutter et al.

1998; Schmidt et al. 1998) have been pursuing cosmology via supernovae surveys, and preliminary results from both groups argue for a nonzero cosmological constant.

The apparent brightness of a standard candle, at a given redshift, is a function not only of the Robertson-Walker model describing the universe, but also of the distribution of matter within the universe. To date, the cosmology results in the literature derived from observed supernovae peak brightnesses are based upon the assumption that the matter in the universe is homogeneously distributed. An important question is to what extent the matter inhomogeneities we see (in the form of galaxies, stars, MACHOs, etc.) affect one's ability to draw conclusions from the data.

It is well known that weak gravitational lensing can impact the degree to which high-redshift supernovae can be considered standard candles, contributing “errors” on the order of 0.05 mag by redshift of one for reasonable cosmologies (Kantowski, Vaughan, & Branch 1995; Frieman 1997; Wambsganss, Cen, Xu, & Ostriker 1998; Holz & Wald 1998; Kantowski 1998a, 1998b). These errors can be beaten down through statistics, since, given a large enough sample of supernovae at a given redshift, the average flux of the supernovae should be representative of the true flux in a pure Robertson-Walker universe. In addition, work has also been done analyzing the high-magnification tail of the lensing distribution, and the information this yields about the distribution of mass inhomogeneities (Schneider & Wagoner 1987). In contrast, the present paper examines the low-magnification part of the lensing distribution, and explores the systematic errors due to the non-gaussian peak. A similar study has been undertaken by Kantowski (1998a, 1998b), examining fits to analytic distance-redshift relations from Swiss-Cheese model universes. In this paper we emphasize the limiting (empty-beam) lensing scenario, and in particular, we use these expressions to directly comment upon current results from supernovae surveys.¹

2. DISTANCE-REDSHIFT RELATIONS

The luminosity of an image, as a function of redshift, is related to the angular diameter distance to the source generating the image. Two common angular diameter distance-redshift relations are given by the filled and empty-beam expressions (Dyer & Roeder 1972, 1973; Fukugita et al. 1992), where in the filled-beam case the line-of-sight to the source traverses mass of exactly the Robertson-Walker density, while in the empty-beam case the beam encounters no curvature (i.e., passes through vacuum, far from all matter distributions). Current analyses of high- z supernovae data use filled-beam expressions to infer the physical distances of the sources from their observed apparent brightnesses (Perlmutter et al. 1998; Riess et al. 1998a). When calculating how far a source is, based upon the brightness of its image, it is therefore assumed that the photon

¹The results discussed in this paper for the case of “standard candles” apply equally well to “standard rulers”. For example, the work of Guerra & Daly (1998) utilizes double radio sources to measure cosmological parameters, arriving at results similar to those of the supernovae groups. Lensing causes apparent lengths to appear systematically shorter, and thus engenders similar effects to those in the supernovae case.

beams pass through exactly the Robertson-Walker mass density. If, for example, the photon beams avoid most of the matter, then a more accurate description would be the empty-beam expressions. By assuming a filled-beam expression in this case, one takes an image dimmed because of the lack of matter in the beam, and concludes from the observed brightness of this image that the source is further away than it really is. With increasing redshift, the differences between the filled and empty-beam brightnesses increase. In this way, evidence of an inhomogeneous universe might be mistaken for evidence of an accelerating one.

The filled and empty-beam distance-redshift relations reduce to the same form for low z , and thus measurements of cosmological parameters from supernovae with statistical weight at lower redshifts will not be affected by lensing. As one moves to higher redshifts, however, the differences between the two expressions can be dramatic. For example, at $z = 1$ a standard candle described by the filled-beam expression in a smooth Robertson-Walker universe, with $\Omega_m = 0.5$, $\Omega_\Lambda = 0.5$, will have the same apparent brightness as a standard candle described by the empty-beam expression in an inhomogeneous universe, with $\Omega_m = 0.5$, $\Omega_\Lambda = 0$. Therefore, based solely upon observations of standard candles at both low redshifts and at a single high redshift, it would be impossible to conclude whether dimming was due to lensing effects or a nonzero cosmological constant. Knowledge of the distance-redshift curve at a range of intermediate to high redshifts is thus crucial.

3. MAGNIFICATION DISTRIBUTIONS

We generate magnification distributions utilizing a recently-developed method to determine lensing statistics in inhomogeneous universes (Holz & Wald 1998). In brief, the method arrives at statistical lensing information by combining aspects from ray-tracing and Swiss-Cheese model numerical approaches. The universe is decomposed into comoving spherical regions, with arbitrary mass inhomogeneities allowed within each region. Statistics are developed by considering many random rays in a Monte-Carlo fashion, and integrating the geodesic deviation equation along each ray in turn. It should be emphasized that this method calculates the lensing effects in full generality, treating both weak and strong lensing effects automatically.

Some representative magnification distributions are shown in Figure 1, for two different matter distributions. The “point mass” panels give the magnification distributions when most of the matter in the universe is in highly condensed objects with masses $\gtrsim 0.01 M_\odot$ (stars, MACHOs, etc.). These results are independent of the mass distribution and clustering of the point masses (Holz & Wald 1998). At the redshifts being considered, point mass lensing will in general be dominated by a single lens encounter, and two images will be generated. The numerical method we utilize generates statistics for uncorrelated photon beams, and thus does not identify the two images associated with a given source (Holz & Wald 1998). However, using analytic expressions for the relative brightnesses of these images (Schneider, Ehlers, & Falco 1992), we are able to convert the magnification distribution for the beams that have not passed through a caustic (which

correspond to the brighter image of a pair) into a magnification distribution for the combined images. The “point mass” panels of Figure 1 show this combined magnification distribution.

For continuous matter distributions, as in the case of isothermal galaxies, the incidence of multiple imaging at the redshifts being considered is highly improbable (<0.2% at $z = 1$ (Holz, Miller, & Quashnock 1998)). In this case strong lensing is unimportant, and weak lensing dominates the results. In the “isothermal” panels of Figure 1, we have taken all of the matter in the universe to be in galaxies, where a galaxy is represented as a truncated isothermal sphere of continuously distributed matter. We take a galaxy number density of $0.025 h^3 \text{ Mpc}^{-3}$ (Geller et al. 1997), which, for a given cosmology, fixes the mass of the galaxies. Taking $\Omega_m = 0.5$ and $H_0 = 65 \text{ km/s Mpc}^{-1}$, the mass of the galaxies is fixed at $8.5 \times 10^{12} \text{ M}_\odot$. If we then take the velocity dispersion of the galaxies to be 220 km/s, the physical truncation radius of the isothermal spheres is set at 380 kpc.

A key feature of the magnification distributions plotted in Figure 1 is that they are non-gaussian. The average of the distributions is given by the Robertson-Walker (filled-beam) value ($\mu = 1$). In all cases, however, the magnification distributions are strongly peaked at values considerably less than this average. Another important characteristic of the distributions is that there is a lower cutoff, given by the empty-beam value, to the possible observed de-magnification. In general, the peak of the magnification distribution will lie somewhere in between the empty and filled-beam values.

With good statistics it may become possible to measure the magnification distribution of the supernovae from observations, and thus determine the matter distribution (Metcalf 1998; Wiegert & Frieman 1998).² In the case of low statistics, as is found in the high- z supernovae surveys, the likelihood of evenly sampling the probability distribution is low. One therefore would expect these surveys to find a “mean” in rough agreement with the (de-magnified) *peak* of the distribution, rather than the average. In the point mass case, the magnification distribution is sharply peaked very near the empty-beam limit, and therefore the empty-beam value is an excellent approximation to the distribution. For continuous matter distributions, such as extended galactic structures, the peak of the distribution is still considerably de-magnified from the filled-beam value: in all the plots of Figure 1 the peak is at least as close, if not closer, to the empty-beam value. Therefore, in the case of extended matter distributions, doing an analysis with the empty-beam expressions in addition to the filled-beam ones serves to bracket the possible range of lensing effects. With this in mind, in the following section we analyze some high- z supernovae data, fitting to empty-beam, as well as the more traditional filled-beam, distance-redshift relations.

² In this manner, a cosmological MACHO experiment is possible. For example, if most of the matter is distributed in point masses, then the peak of the magnification distribution will be very near the empty-beam value. In this case, there will be little fluctuation to brightness values dimmer than the mean, and considerably more fluctuation to brighter values. In addition, this asymmetry will grow with redshift in a well defined manner. It is to be stressed that these MACHO detections are possible even without strongly magnified supernovae or time-dependent lensing effects.

4. APPLICATION TO SUPERNOVAE DATA

We use a sample of supernovae as a testbed to determine the qualitative effects of lensing on high- z supernovae surveys. To this end, we take distance data for a total of 37 supernovae from the high- z supernovae team: 27 supernovae at $0.01 \lesssim z \lesssim 0.1$ (Hamuy et al. 1996), and ten higher-redshift supernovae reported in Riess et al. (1998a) (and analyzed using the MLCS method of Riess, Press, & Kirshner (1996)), including SN97ck at $z = 0.97$ (Garnavich et al. 1998).

For the low-redshift sample, we take the distance errors listed in Table 10 of Riess et al. (1998a), and the dispersion in host galaxy redshifts (due to peculiar velocities and other uncertainties) to be 200 km/s. For the high- z sample, we take the errors listed in Riess et al. (1998a). We find that the fits are not sensitive to the particular error values, in agreement with Riess et al. (1998a).

We fix the Hubble constant to be 65 km/s Mpc^{-1} , in accord with the determination of Riess et al. (1998a). As H_0 is determined from supernovae (or other methods) at low redshifts, gravitational lensing is not expected to affect this result. Furthermore, it should be stressed that all of the results discussed in this paper are independent of the value of H_0 .

In parallel with § 4.1 of Riess et al. (1998a), we do a two parameter $(\Omega_m, \Omega_\Lambda)$ minimum χ^2 fit, neglecting regions with $\Omega_m < 0$, and other unphysical regions (“no big bang” regions (Carroll, Press, & Turner 1992)). The Hubble-diagram for the data set is shown in the top panel of Figure 2, plotted against the best-fit (minimum χ^2) curve. The bottom panel plots the residual Hubble diagram (where the $\Omega_m = \Omega_\Lambda = 0$ magnitudes have been subtracted out). The best fit curve is a model with $\Omega_m = 0, \Omega_\Lambda = 0.45$ ($\chi^2_\nu = 1.15$, for 35 degrees of freedom). This is in good agreement with the result of Riess et al. (1998a) ($\Omega_m = 0, \Omega_\Lambda = 0.48$ ($\chi^2_\nu = 1.17$)), which comes from an identical set of supernovae, but with updated MLCS values (Riess et al. 1998b). Both empty and filled-beam models find this value (which is identical in each case) as their best fit. Note that the data points in the bottom panel trend towards values above the axis, indicating a nonzero cosmological constant, regardless of lensing. Also note that the models become most clearly separated at high- z , and therefore the discretionary power lies in the few highest-redshift supernovae. This can readily be seen by the striking contrast between contours from Perlmutter et al. (1997) and those from Perlmutter et al. (1998), where the latter paper includes the addition of a single supernova at $z = 0.83$. The more sensitive the fits are to the highest- z supernovae, the more lensing effects can come into play.

Although the empty and filled-beam cases agree on a best-fit model, in neither case is the fit particularly tight. Therefore it is particularly informative to consider likelihood contours, as discussed in Riess et al. (1998a). By integrating over successive regions of $(\Omega_m, \Omega_\Lambda)$ phase space, we are able to determine the values of χ^2 corresponding to the 68%, 95%, and 99.7% confidence boundaries (representing 1σ , 2σ , and 3σ regions of fit, respectively). Figure 3 shows contours of constant χ^2 representative of these 1σ , 2σ , and 3σ confidence intervals, for the filled-beam case (background shaded contours), and the empty-beam case (foreground dashed contours). The filled

and empty-beam contours are very similar near the $\Omega_m = 0$ axis, where there is little matter to cause lensing. As one progresses to models with more significant matter content, the empty-beam contours remain wider than the filled-beam counterparts, closing off at much larger Ω_m and Ω_Λ values. Thus the inclusion of lensing broadens the class of consistent cosmological models. Furthermore, the empty-beam contours drift downwards: the empty-beam fits prefer higher values of Ω_m , and lower values of Ω_Λ . These results appear to agree with preliminary results from the Supernovae Cosmology Project (Aldering 1998).

5. CONCLUSIONS

We have argued that lensing will systematically skew the peak of the apparent brightness distribution of supernovae away from the filled-beam value and towards the empty-beam value. Even in the case of continuous mass distributions, the peak is expected to be closer to the empty-beam value than the filled-beam value.

Based upon our results from a limited number of supernovae data points, some qualitative statements regarding the impact of lensing on the determination of cosmological parameters from high- z supernovae surveys can be made. For universes with little or no Ω_m , the impact of lensing is slight, as Λ dominates the apparent brightness. As the current data samples seem to favor vacuum models, lensing will not generally affect their best fits. However, the error ellipses undergo significant changes due to the inclusion of lensing, favoring models with lower values of Ω_Λ and higher values of Ω_m . For example, the empty-beam best fit flat model ($\Omega_m + \Omega_\Lambda = 1$) has $\Omega_m = 0.32$ ($\chi^2 = 1.155$). This fit is essentially as good as the overall best fit ($\Omega_m = 0$, $\Omega_\Lambda = 0.45$ ($\chi^2 = 1.152$)). The filled-beam best fit flat model has $\sim 25\%$ less matter ($\Omega_m = 0.26$), and is a slightly worse fit ($\chi^2 = 1.161$).

Currently the true best fit to the data finds negative values for Ω_m . As we neglect $\Omega_m < 0$ on physical grounds, the likelihood contours are squashed up against the $\Omega_m = 0$ axis, causing the differences between empty and filled-beam fits to be small. Should future data favor a positive value of Ω_m , much greater differences between the empty and filled-beam contours are to be expected.

The author wishes to thank Don Lamb, Mike Turner, and especially Bob Wald for valuable discussions in the course of this work. The author also wishes to acknowledge Warner Miller for the initial stimulus to undertake this project. This work was supported by NSF grant PHY 95-14726.

REFERENCES

Aldering, G. 1998, private communication

Carroll, S. M., Press, W. H., and Turner, E. L. 1992, *ARA&A* 30, 499

Dyer, C.C. & Roeder, R.C. 1972, *ApJ*, 174, L115

———. 1973, *ApJ*, 180, L31

Frieman, J. A. 1997, *Comments Astrophys.*, 18, 323; astro-ph/9608068

Fukugita, M., Futamase, T., Kasai, M., & Turner, E. L. 1992, *ApJ*, 393, 3

Garnavich, P., et al. 1998, in preparation

Geller, M. J. et al. 1997, *AJ*, 114, 2205; astro-ph/9710109

Guerra, E. J. 1998, *ApJ*, 493, 536

Hamuy, M. et al. 1996, *AJ*, 112, 2398; astro-ph/9609062

Holz, D. E., Miller, M. C., & Quashnock, J. M. 1998, submitted to *ApJ*; astro-ph/9804271

Holz, D. E., & Wald, R. 1998, *Phys. Rev. D*, in press; astro-ph/9708036

Kantowski, R. 1998a, astro-ph/9802208

———. 1998b, astro-ph/9804249

Kantowski, R., Vaughan, T., & Branch, D. 1995, *ApJ*, 447, 35

Metcalf, R. B. 1998, astro-ph/9803319

Perlmutter, S. et al. 1997, *ApJ*, 483, 565

Perlmutter, S. et al. 1998, *Nature* 391, 51

Premadi, P., Martel, H., & Matzner, R., *ApJ* 493, 10

Riess, A. G., Press, W. H., & Kirshner, R. P. 1996, *ApJ*, 473, 88

Riess, A. G. et al. 1998a, to appear in *AJ*; astro-ph/9805201

Riess, A. G. et al. 1998b, in preparation

Schmidt, B P. et al. 1998, to appear in *ApJ*; astro-ph/9805200

Schneider, P., Ehlers, J., and Falco, E. E. 1992, *Gravitational Lensing* (Berlin: Springer)

Schneider, P. & Wagoner R. V. 1987, *ApJ* 314, 154

Turner, E. L., Ostriker, J. P., & Gott, J. R. 1984, *ApJ*, 284, 1

Wambsganss, J., Cen, R., Xu, G. & Ostriker, J. P. 1997, *ApJ*, 475, L81

Wiegert, C. & Frieman, J. A. 1998, in preparation

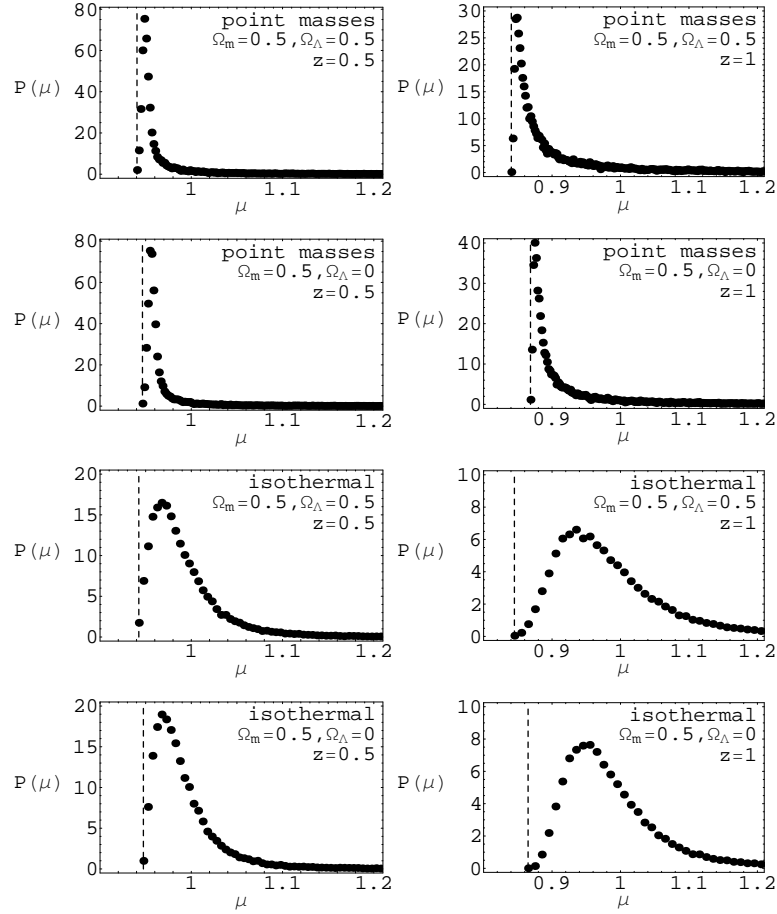


Fig. 1.— Probability distribution, $P(\mu)$, for supernovae apparent brightness, μ , normalized so that $\mu = 1$ corresponds to the filled-beam, or homogeneous Robertson-Walker, value. The vertical dashed lines are at the empty-beam value. The brightness distributions are at $z = 0.5$ and $z = 1$, for the models as indicated. The point mass distribution represents the case where all of the matter is in compact objects. The isothermal distribution is for matter in galaxies, represented as isothermal spheres with truncation radii 380 kpc.

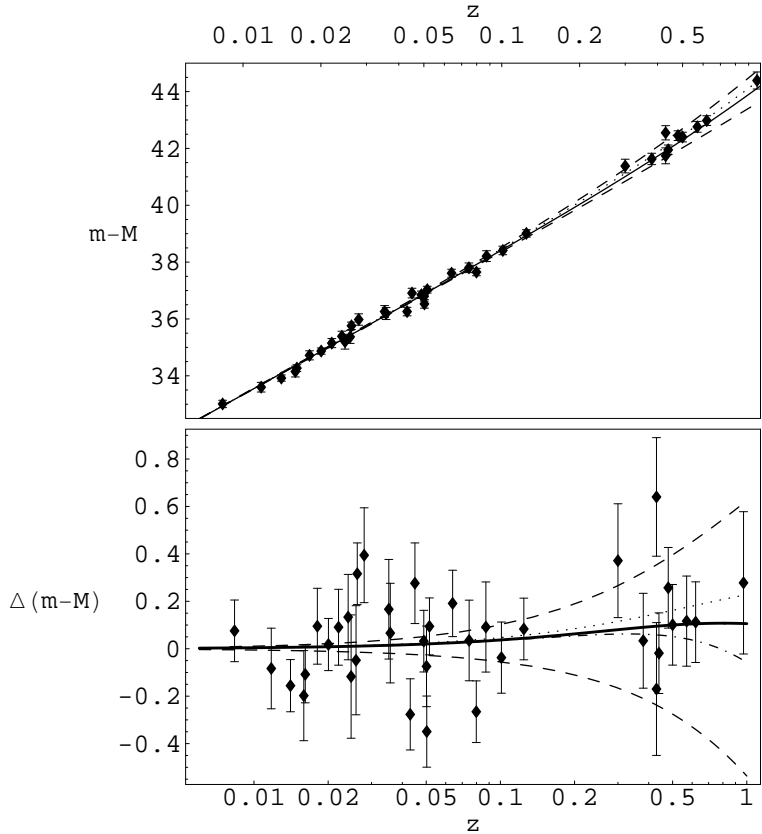


Fig. 2.— The Hubble diagram, with both theoretical distance–redshift relations and supernovae data plotted. The upper panel shows the traditional Hubble diagram, with filled-beam distance–redshift relations. The top (dashed) curve is for an $\Omega_m = 0, \Omega_\Lambda = 1$ model. The bottom (dashed) curve is for an $\Omega_m = 1, \Omega_\Lambda = 0$ model. The solid curve is the fiducial $\Omega_m = \Omega_\Lambda = 0$ case. The dotted curve is the best fit to the data, corresponding to $\Omega_m = 0, \Omega_\Lambda = 0.45$. The bottom panel shows a residual Hubble diagram, with the values of the $\Omega_m = \Omega_\Lambda = 0$ model subtracted from the data. The same curves as in the upper panel are shown. Two additional curves are also plotted: the solid curve is the empty-beam distance–redshift relation for $\Omega_m = 0.4, \Omega_\Lambda = 0.6$. The dot-dashed curve is the filled-beam relation for the same parameters. Note that the empty-beam $\Omega_m = 0.4, \Omega_\Lambda = 0.6$ case is essentially as good as the best fit ($\chi^2_\nu = 1.17$), while the corresponding filled-beam case is well over 1σ away ($\chi^2_\nu = 1.24$).

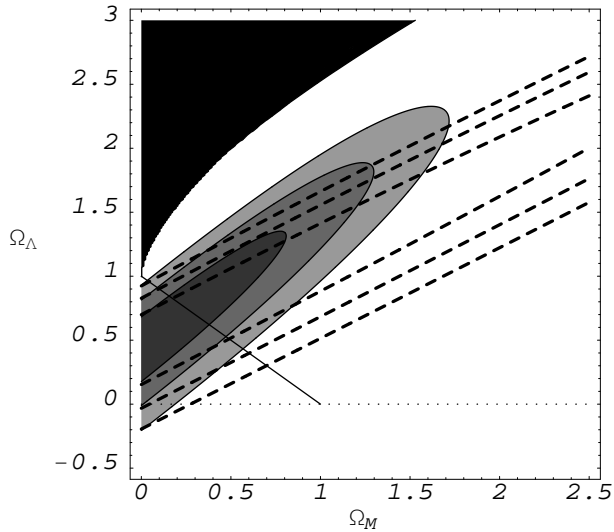


Fig. 3.— Contours of constant χ^2 in $(\Omega_m, \Omega_\Lambda)$ parameter space, for the SNe data set of Fig. 2. The background shaded contours correspond to the 68%, 95%, and 99.7% joint confidence intervals in the filled-beam case. The dashed lines correspond to the same confidence regions in the empty-beam case. The dotted line represents $\Lambda = 0$ cosmologies, while the diagonal line represents $\Omega_m + \Omega_\Lambda = 1$ cosmologies. The blackened region at the upper left is excluded (no big bang).